International Journal of Bifurcation and Chaos, Vol. 24, No. 8 (2014) 1440004 (20 pages)

DOI: 10.1142/S0218127414400045

Symbolic Quest into Homoclinic Chaos

Tingli Xing
Department of Mathematics and Statistics,
Georgia State University, Atlanta 30303, USA
txing1@student.gsu.edu

Roberto Barrio
Departamento de Matemática Aplicada and IUMA,
University of Zaragoza, E-50009, Spain
rbarrio@unizar.es

Andrey Shilnikov
Neuroscience Institute and
Department of Mathematics and Statistics,
Georgia State University, Atlanta 30303, USA
Department of Computational Mathematics and Cybernetics,
Lobachevsky State University of Nizhny Novgorod,
Nizhny Novgorod 603950, Russia
ashilnikov@gsu.edu

Received February 2, 2014

In Memoriam of Leonid Pavlovich Shilnikov

We explore the multifractal, self-similar organization of heteroclinic and homoclinic bifurcations of saddle singularities in the parameter space of the Shimizu–Morioka model that exhibits the Lorenz chaotic attractor. We show that complex transformations that underlie the transitions from the Lorenz attractor to wildly chaotic dynamics are intensified by Shilnikov saddle-foci. These transformations are due to the emergence of Shilnikov flames originating from inclination-switch homoclinic bifurcations of codimension-two. We demonstrate how the original computational technique, based on the symbolic description and kneading invariants, can disclose the complexity and universality of parametric structures and their link with nonlocal bifurcations in this representative model.

Keywords: Shilnikov saddle-focus; Shilnikov flame; chaos; homoclinic orbit; heteroclinic orbit; Lorenz attractor; wild chaos; strange attractor; kneading invariant; symbolic dynamics; T-point; codimension-two bifurcation.

1. Introduction

The iconic shape of the Lorenz attractor has long been an emblem of Chaos theory as a new paradigm in nonlinear sciences. This emblem has been reprinted innumerable times on posters announcing popular lectures and professional meetings with cross-disciplinary scopes, and/or with particular emphasis on dynamical systems and bifurcations. The concept of deterministic chaos illustrated by snapshots of the Lorenz attractor has been introduced in all modern textbooks on nonlinear dynamics. Nowadays, its butterfly-shaped image is stereotypically associated with images of deterministic chaos as a whole.

The library of publications on systems with the Lorenz attractor has considerably grown over a half century, since the celebrated paper [Lorenz, 1963] came out introducing a basic system of three ordinary differential equations with highly unordinary trajectory dynamics.

The ideas of this research trend are deeply rooted in the pioneering studies led by L. P. Shilnikov in the city of Gorky, USSR [Shilnikov, 1980; Afraimovich *et al.*, 1977, 1983; Bykov, 1980]. He was a creator of the theory of homoclinic bifurcation and a founder of the theory of strange attractors. His extensive knowledge of global bifurcations helped to turn chaos theory into a mathematical marvel [Shilnikov, 1967b, 1968b, 1981, 1994, 1997, 2002; Afraimovich & Shilnikov, 1983; Turaev & Shilnikov, 1998]. His contributions to the theory are pivotal and include the identification and description of the structures of bifurcation routes to spiral and screw-like strange attractors emerging through bifurcations of the famous Shilnikov saddle-focus [Shilnikov, 1965, 1967a, 1970], which have been found in a broad range of applications from nonlinear optics to biology and finance. He proposed scenarios of the onset of chaos through a torus breakdown [Afraimovich & Shilnikov, 1974, 1991], the onset of complex dynamics caused by structurally unstable homoclinics of saddle periodic orbits [Gavrilov & Shilnikov, 1972, 1973], as well as that of shift dynamics after the disappearance of a Shilnikov saddle-node, also called a saddle-saddle [Shilnikov, 1969; Shilnikov & Shilnikov, 2008]. Concerning the Lorenz attractor, he pointed out the conditions sufficient for a system to possess the Lorenz attractor [Afraimovich *et al.*, 1983]. These conditions were used to verify and to determine the existence regions of the Lorenz attractor, and to present computer assisted proofs of chaotic dynamics without stable orbits and homoclinic tangencies in the canonical Lorenz model [Sinai & Vul, 1981; Bykov & Shilnikov, 1992; Tucker, 1999].

In his PhD thesis, L. P. Shilnikov proved the generalizations of homoclinic bifurcations of a saddle and a saddle-node, which lead to the emergence of a stable periodic orbit in $\mathbb{R}^n$, $n \geq 3$ [Shilnikov, 1962, 1963]. Having defended it, his interest wholly switched from systems with trivial dynamics and their spatial generalizations to a brand new challenge that he had set for himself — high-dimensional systems with complex, structurally unstable dynamics — the precursors of deterministic chaos. In 1968, L. P. Shilnikov published a paper proving the existence and uniqueness of a saddle periodic orbit emerging through a homoclinic bifurcation of a saddle in $\mathbb{R}^3$ and higher dimensions [Shilnikov, 1968a]. In this paper, he introduced the conditions giving rise to the novel bifurcations of codimension-two termed as orbit-flip and inclination-switch (Fig. 3).[1] This result (as well as ones above, treated as scientific folklore, i.e. without acknowledging his original papers), along with the widely-known Shilnikov saddle-focus [Shilnikov, 1965, 1967a, 1970] and a less known Shilnikov saddle-node [Shilnikov, 1969; Shilnikov & Shilnikov, 2008], constituted his thesis for a degree of Doctor of Science. The degree was never granted because of intrigues of his former graduate tutor Y. I. Neimark, who had managed his network connections within the Soviet science establishment to obstruct such an original and independent researcher as L. P. Shilnikov at 35 years old. That unfortunate episode did not affect his stellar career of an academician, so Shilnikov had never considered a reapplication for that degree. Mid 1970's and early 80's were just the beginning of his new era of qualitative theory of differential equations and bifurcations with the emphasis upon complex dynamics, the field that is known today as the advanced theory of dynamical systems.

In this paper, we would like to rediscover the wonder of systems with Lorenz-like attractors, which are viewed not only through the prism of the elegant complexity of the trajectories' behavior in the phase space, but also by disclosing a plethora of generic fractal-hierarchical organizations of the parameter space. Our work is aimed at illustrating the richness of homoclinic bifurcations underlying the magic metamorphoses of chaos in the exemplary Shimizu–Morioka models and like systems. It is an extension of the ideas introduced in the earlier paper "Kneadings, Symbolic Dynamics and Painting Lorenz Chaos" by R. Barrio, A. L. Shilnikov and L. P. Shilnikov [Barrio *et al.*, 2012]. The original computational approaches that we have been developing for studying systems with complex dynamics capitalize

[1]Upon fulfillment of certain conditions these bifurcations can lead to the onset of complex dynamics in Z_2-symmetric systems, specifically, to the appearance of the Lorenz attractor [Shilnikov, 1981].

on the key property of deterministic chaos — the sensitive dependence of solutions in such a system on variations of bifurcation parameters. In particular, for the Lorenz-type attractors, chaotic dynamics are characterized by unpredictable flip-flop switching between the two spatial wings of the strange attractor, separated by a saddle singularity at the origin in the phase space.

2. The Shimizu–Morioka Model

The three-parameter extension of the Shimizu–Morioka (SM) model [Shimizu & Morioka, 1980; Shilnikov, 1986, 1989, 1991] is given by

$$\dot{x} = y, \quad \dot{y} = x - \lambda y - xz - Bx^3, \\ \dot{z} = -\alpha(z - x^2); \tag{1}$$

here, $\{\alpha, \lambda > 0\}$ are the primary bifurcation parameters. Equations (1) are known to be a normal form for triple-degenerate equilibria and periodic orbits in a Z_2-symmetric central manifold [Shilnikov *et al.*, 1993; Vladimirov & Volkov, 1993]. Moreover, the Lorenz model can be reduced to Eqs. (1) with proper parameter and coordinate substitutions [Petrovskaya & Yudovich, 1980]. We will start with the classical case $B = 0$, and later use its variation to globally unfold the bifurcation structures. Like the Lorenz equation, this symmetric model, i.e. $(x, y, z) \leftrightarrow (-x, -y, z)$, has three equilibrium states: two stable-foci at $(\pm\sqrt{\alpha}, 0, 1)$ that become saddle-foci through an Andronov–Hopf bifurcation, which is supercritical, not sub-, in the given case. The origin is a saddle of (2,1)-type, i.e. with a couple of 1D outgoing separatrices. The type of the saddle is determined by the eigenvalues, $s_3 < s_2 < 0 < s_1$, of the linearization matrix at the origin. The saddle index, being a ratio of the leading eigenvalues $\nu = s_1/|s_2|$, determines the stability and the number of periodic orbits bifurcating from a homoclinic loop. If $\nu > 1$, the only stable periodic orbit can bifurcate from a homoclinic loop [Shilnikov, 1962, 1963]. Though cases with $\nu < 1$ are more delicate, generally there is a single saddle orbit bifurcating from a homoclinic loop unless the outgoing separatrix twists along the loop, or returns to the saddle from the direction due to s_3, instead of leading s_2. These bifurcations are referred to as orbit-flip and inclination-switch in modern literature. A saddle with $\nu = 1$ is called resonant; this homoclinic bifurcation gives rise to a saddle-node periodic orbit. These three primary codimension-two bifurcations were discovered by L. P. Shilnikov in the 1960s [Shilnikov, 1968a; Shilnikov *et al.*, 1998, 2001]. Either bifurcation of the homoclinic butterfly made simultaneously from two homoclinic loops in a $\mathbb{Z}_2$-system can give rise to the onset of the Lorenz attractor [Shilnikov, 1981, 1986; Robinson, 1989; Rychlik, 1990; Shilnikov, 1993; Shilnikov *et al.*, 1993; Tigan & Turaev, 2011]. Of special interest here are codimension-two homoclinic bifurcations of two kinds: the resonant saddle, giving rise to the appearance of the Lorenz attractor and shaping its existence region in the parameter space together with the inclination-switch bifurcations terminating the Lorenz attractor in the SM-model. As we show

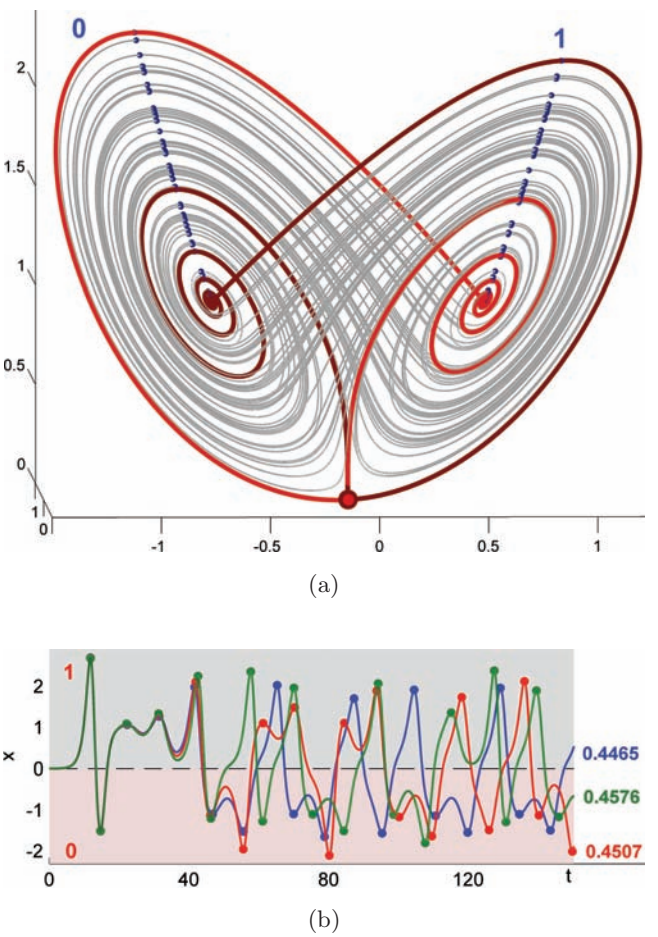

Fig. 1. (a) The (x, z)-projection of a heteroclinic connection (red color) between the saddle (at the origin) and the saddle-foci overlaid with the chaotic attractor (gray color) in the background in the phase space projection on the SM-model at the primary T-point. The flip-flopping of the "right" separatrix defines the binary entries, $\{1, 0\}$, of kneading sequences, depending on whether it turns around the right or left saddle-focus, respectively and (b) sensitivity of time progressions of the separatrix results in kneading sequences with the same initial episode $\{1, 0, 1, 1, 1, 0 \ldots\}$ due to small variations of the λ-parameter.

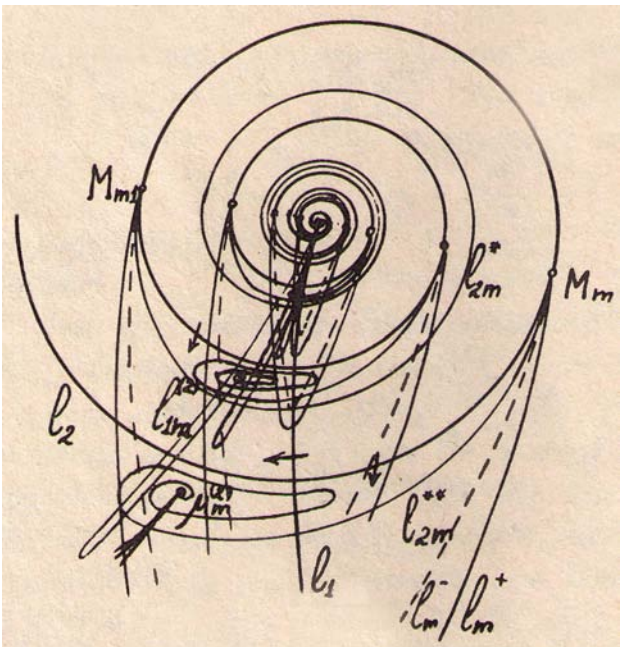

Fig. 2. Sketch of a partial bifurcation unfolding of a Bykov T-point (from [Bykov, 1980]) corresponding to a codimension-two heteroclinic connection between a saddle of the $(2,1)$-type and a saddle-focus of the $(1,2)$-type. It features the characteristic spirals corresponding to homoclinic bifurcations of the saddle. Turning points (labeled by M's) on the spiral are codimension-two points of inclination-switch bifurcations giving rise to stable periodic orbits through saddle-node and period-doubling bifurcations (l_m-curves) and subsequent spiral structures of smaller scales between spiral's scrolls.

below, there is another type of codimension-two points, called Bykov T-points, which are typical for Lorenz-like systems [Bykov, 1980; Glendinning & Sparrow, 1986; Bykov, 1993]. Such a point corresponds to a closed heteroclinic connection between three saddle equilibria [Fig. 1(a)] in Eqs. (1): the saddle at the origin and two symmetric saddle-foci of the $(1,2)$-type. Such points turn out to cause the occurrence of self-similar, fractal structures in the parameter region corresponding to chaotic dynamics in the known systems with the Lorenz attractor [Barrio *et al.*, 2012; Xing *et al.*, 2014a; Xing *et al.*, 2014b].

Figure 4 presents a Lyapunov exponent (LE) based sweep of the parameter space of the model with its attractors superimposed in the color-coded regions. The regions are painted as follows: white, gray and red corresponding to stable equilibrium states, periodic orbits and chaotic dynamics, respectively, in the model. The borderline between the first two should be interpreted as an Andronov–Hopf bifurcation giving rise to stable orbits as the parameter λ is decreased. The red region of chaos has sharp borders too, including a cusp-shaped "beak" with a tip corresponding to a homoclinic butterfly bifurcation of a resonant saddle with the saddle index $\nu = 1$ [Shilnikov, 1986, 1989]. The existence of the homoclinic butterfly in the SM-model was proven in [Tigan & Turaev, 2011]. Last but not least, we note multiple stability islands with stable periodic orbits that occur within the chaotic red region, or cut it through from outside. In what follows we will elaborate, step by step, on the origin and arrangements of global bifurcations organizing the region of chaotic dynamics that only looks homogeneously solid in the LE-sweep(s).

2.1. *Bykov T-points*

Let us first introduce the principle organization for the bifurcation unfolding, sketched in Fig. 2, of

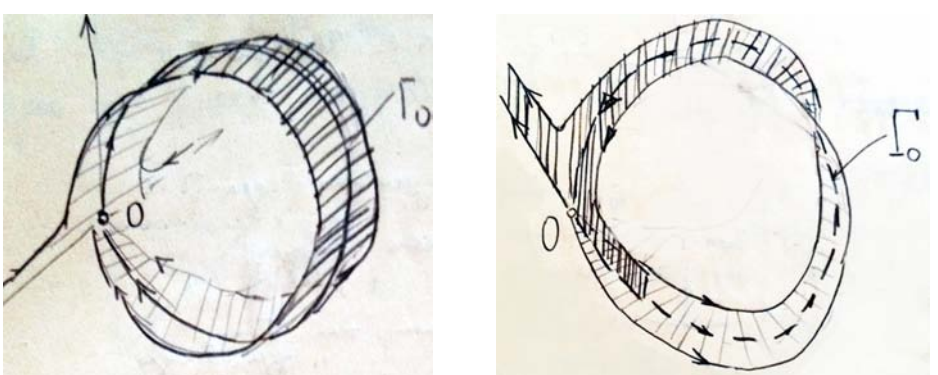

(a) (b)

Fig. 3. L. P. Shilnikov's drawings of an inclination-switch homoclinic bifurcation en route from (a) an orientable to (b) a non-orientable separatrix loop Γ_0 (the median line of a Möbius band) of a saddle O in $\mathbb{R}^3$.

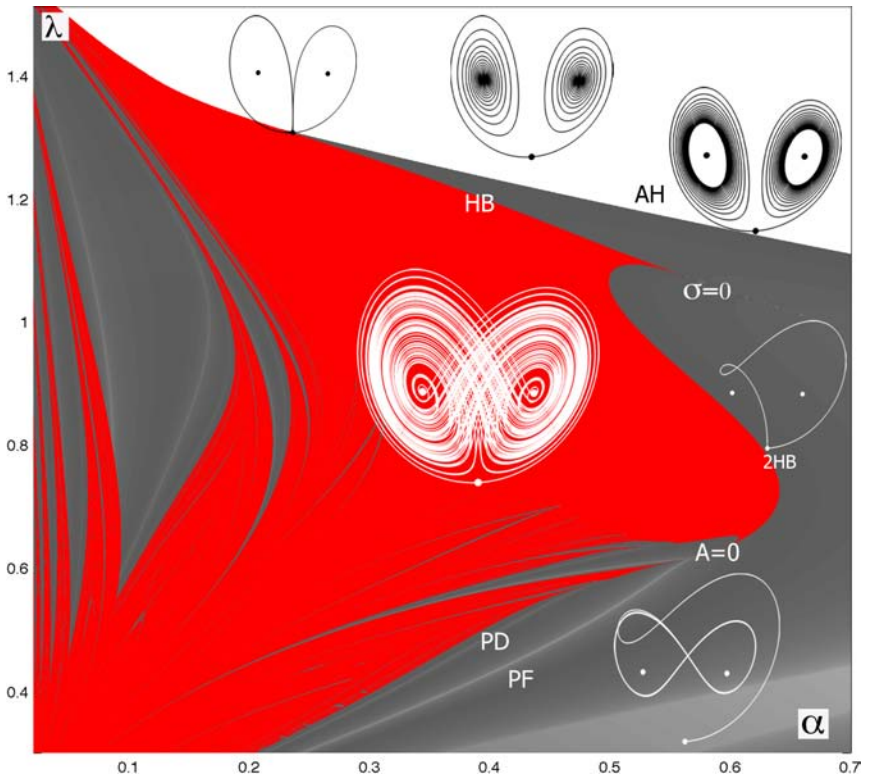

Fig. 4. Bi-parametric sweep of the SM model using Lyapunov exponents (LE): the white, gray and red colors correspond to the existence regions of stable equilibria where the largest LE, $L_1 < 0$, stable periodic orbits where $L_1 = 0$, and chaotic dynamics where $L_1 > 0$. White lines in the gray regions are associated with period-doubling (PD) and pitch-fork (PF) bifurcations at which the second LE, L_2, also reaches zero from below. The borderline between the white and gray regions corresponds to a supercritical Andronov–Hopf bifurcation. Notice a fractal border between regions of chaotic and simple dynamics.

a Bykov T-point corresponding to a closed heteroclinic connection between a saddle-focus and a saddle [Bykov, 1980]. Its characteristic feature is a bifurcation curve spiraling onto the T-point. This curve corresponds to a homoclinic loop of the saddle such that the number of turns of the separatrix around the saddle-focus increases by one with each turn of the spiral approaching the T-point. The line, l_1, originating from the T-point corresponds to homoclinics of the saddle-focus satisfying the Shilnikov condition [Shilnikov, 1965, 1970; Shilnikov & Shilnikov, 2007], and hence leading to the existence of a denumerable set of saddle periodic orbits nearby [Shilnikov, 1967a]. Turning points (labeled by M's) on the primary spiral correspond to inclination-switch homoclinic bifurcations of the saddle [Shilnikov *et al.*, 1993, 1998, 2001]. Each such homoclinic bifurcation point gives rise to the occurrence of saddle-node and period-doubling bifurcations of periodic orbits of the same symbolic representation. The central T-point gives rise to countably many subsequent T-points with similar bifurcation structures on smaller scales in the parameter plane. In addition to the indicated curves in the unfolding of a generic T-point, the unfolding of a T-point in a $\mathbb{Z}_2$-symmetric system has other bifurcation curves, for example, corresponding to heteroclinic connections between both saddle-foci [Bykov, 1980; Glendinning & Sparrow, 1986; Bykov, 1993].

3. Symbolic Description via Kneadings

A hallmark of a Lorenz-like system is a strange attractor in the emblematic butterfly shape [Fig. 1(a)]. The eyes of the butterfly wings demarcate the location of stable foci or saddle-foci. The strange attractor of the Lorenz type is structurally unstable [Guckenheimer & Williams, 1979; Afraimovich *et al.*, 1983] as the separatrices of the saddle at the origin bifurcate constantly as the parameters are varied. These separatrices are the primary cause of structural and dynamic instability of chaos in the Lorenz equations and similar models. We say that the Lorenz attractor undergoes

a homoclinic bifurcation when either separatrix of the saddle changes a flip-flop pattern of switching between the butterfly wings centered around the saddle-foci. At such a bifurcation, the separatrices come back to the saddle, thereby causing a homoclinic explosion in phase space [Afraimovich *et al.*, 1977; Kaplan & Yorke, 1979]. The time progression of either separatrix of the origin can be described symbolically and categorized in terms of the number of turns around two symmetric saddle-foci in the 3D phase space [Fig. 1(a)]. Alternatively, the problem can be reduced to the time progression of the x-coordinate of the separatrix [Fig. 1(b)]. In symbolic terms the progression of the separatrix can be described through a binary (e.g. $1, 0$) alphabet *per se*. Namely, each turn of the separatrix around the right or left saddle-focus, is associated with either 1 or 0, respectively. For example, the time series shown in Fig. 1(b) generates the kneading sequences starting with $\{1, 0, 1, 1, 1, 0 \ldots\}$ at close parameter values. Thus, to differentiate between complex dynamics near a point of interest, one may want to skip an initial episode of kneading sequences to focus on their tails. Clearly, the sequences corresponding to chaotic dynamics will fluctuate unpredictably as the parameters vary.

The core of the computational toolkit is the binary $\{0, 1\}$ representation of a single solution — the outgoing separatrix of the saddle as it fills out the two spatiality symmetric wings of the Lorenz attractor at different parameter values. Such patterns can persist or change with variations of the parameters of the system. Realistically, and numerically, we can assess and differentiate between only appropriately long episodes of patterns, initial or intermediate, due to resolution limits. A positive quantity, called the kneading [Milnor & Thurston, 1988], bearing information about the pattern, allows one to quantify the dynamics of the system. By sweeping bi-parametrically, we create a map of the kneadings. Knowing the range of the kneading, we color-map the dynamics of the system in question onto the parameter plane. Whenever particular kneading quantity persists with variations of control parameters, then the flip-flop pattern does not change, thus indicating that dynamics can be robust (structurally stable) and simple. The straight forward application of this approach nevertheless fails to detect bifurcations, such as period-doubling and pitch-fork of periodic orbits. While this can still be remedied, these bifurcations are not a prime focus of this study elaborating on homoclinic bifurcations and how they can transform the Lorenz attractor.

In the parameter region of the Lorenz attractor, the flip-flop patterns change constantly and unpredictably. Nevertheless, a kneading value remains the same along a level curve. Such a curve corresponds to a homoclinic bifurcation of two separatrix loops of some configuration symbolically and uniquely described by the binary alphabet. No such bifurcation curves may cross or merge unless at a singular point corresponding to some homo- or heteroclinic bifurcation of codimension-two in the parameter plane of the model. As such, by foliating the parameter plane with such multicolored lines, one can reveal the bifurcation structures and identify organizing centers — the singular points.

The kneading invariant was originally introduced to uniquely quantify the complex dynamics described by two symbols in a system, such as, for example, 1D logistic or skew-tent maps with increasing and decreasing branches separated by a critical point. Such maps emerge in a large number of dissipative systems including ones with Lorenz-like attractors. Moreover, such systems can be topologically conjugated if they bear the same kneading invariant [Rand, 1978; Malkin, 1991; Tresser & Williams, 1993]. Without finding 1D maps, a kneading sequence $\{\kappa_n\}$ can be directly generated by time progressions of, say, the right separatrix, Γ^+, of the saddle, using the following rule:

$$\kappa_n = \begin{cases} 1, & \text{when } \Gamma^+ \text{ turns around } O_{\text{right}}, \\ 0, & \text{when } \Gamma^+ \text{ turns around } O_{\text{left}}. \end{cases} \tag{2}$$

The kneading invariant is defined in the form of a formal power series

$$K(q, \mu) = \sum_{n=0}^{\infty} \kappa_n q^n, \tag{3}$$

convergent for $0 < q < 1$. The kneading sequence $\{\kappa_n\}$ comprised of only 1's corresponds to the right separatrix, Γ^+ converging to an equilibrium state or an orbit with $x(t) > 0$. The corresponding kneading invariant is maximized at $\{K_{\max}(q)\} = 1/(1-q)$. When the separatrix converges to an ω-limit set with $x(t) < 0$, then the kneading sequence begins with the very first 1 followed only by 0s. Skipping the very first "1", yields the range, $[0, q/(1-q)]$, of the kneading invariant values; at $q = 1/2$, it is $[0, 1]$.

For each model, one has to figure an optimal value of q: setting it too small makes the convergence too fast so that the tail of the series would have little significance and hence would not differentiate fine dynamics of the system on longer time scales. Note that $q = 1/2$ is the largest value that guarantees the one-to-one correspondence between the time progression of the separatrix and the value of kneading invariant, K.

Given the range and the length of the kneading sequence, a colormap of a preset resolution is defined to provide the conversion of a numeric value of the kneading invariant into a unique color. In this study, the colormap includes 100 different colors chosen so that any two close kneadings are represented by contrasting hues. Specifically, the colormap is given by a 100×3 matrix, the columns of which correspond to [RGB] values standing for the red, green, and blue colors represented by $\{100\}$, $\{010\}$ and $\{001\}$, respectively. The R-column of the colormap matrix has entries linearly decreasing from 1.0 to 0.0, the B-column has entries linearly increasing from 0.0 to 1.0, while any entry of the G-column alternates between 0 and 1 to produce color diversities. So, by construction, the blue color represents kneading invariants in the $\{0.99, 1.0\}$ range, the red color on the opposite side of the spectrum corresponds to kneading invariants in the $\{0, 0.01\}$ range, and all other 98 colors fill the spectrum in between. A borderline between two colors corresponds to a homoclinic bifurcation of the saddle through which the kneading invariant changes its value. Due to resolution, the colormap is sensitive only to variations of the first two decimals of the kneading value. For this reason we only consider kneading sequences of length 10, with the maximal contribution of the tail about $0.5^{11}/(1 - 0.5) = 0.5^{10} \approx 10^{-3}$ to the kneading value. To obtain finer structures of the bifurcation diagram foliated by longer homoclinic loops, one should skip a number of initial kneadings to keep episodes 10 entries long or so: {3–12}, {22–31}, and so forth. Such a sweep can reveal up to 2^{10} distinct homoclinic bifurcations. A word of caution: having information in excess, i.e. overwhelmingly many bifurcation curves of random colors, will make the bifurcation diagram look noisy on the large scale even though the number of mesh points is large enough. Producing clear and informative diagrams for the given system takes time and some amount of experimental work.

4. Symbolic Sweeping: Swirls and Saddles

The bi-parametric, (α, λ)-scan of Eqs. (1) at $B = 0$ using the {5–15} kneading range is presented in Fig. 5. This high-resolution diagram is made of 40 panels, each with $10^3 \times 10^3$ mesh points. A region of a solid color corresponds to a constant kneading invariant, i.e. to structurally stable and simple dynamics in the system. In such regions, trivial attractors, such as stable equilibria or stable periodic orbits, dominate the dynamics of the model. The red, blue and light blue colors correspond to constant values of the kneading invariants: 0, 1 and 2/3 generated, respectively, by sequences $\{0\}^\infty$, $\{1\}^\infty$ and $\{10\}^\infty$. Note that the kneading approach does not distinguish between symmetric and asymmetric periodic orbits, for instance, of the figure-eight shape generating the same sequence $\{10\}^\infty$. As such it does not detect pitch-fork and period-doubling bifurcations.

A borderline between two solid-color regions corresponds to a homoclinic bifurcation at which the kneading invariant becomes discontinuous and experiences a sudden jump in its value. So, the border between the blue (the kneading invariant $K = 1$) and the red ($K = 0$) regions corresponds to the bifurcation curve, HB, of the primary homoclinic butterfly. The same curve is continued as a borderline between the blue and light blue regions. The point where all three regions come together on the bifurcation curve corresponds to the resonant saddle with $\nu = s_1/|s_2| = 1$, or with zero saddle value: $\sigma = s_2 + s_1 = 0$. To the right of it, the homoclinic bifurcation with $\sigma < 0$ "glues" two stable periodic orbits, emerging from stable foci through a supercritical Andronov–Hopf curve, AH, into a single orbit (x, y)-projected as a figure-eight (Fig. 5). To the left, the codimension-two point, $\sigma = 0$ ($\nu = 1$) originates a loci (bundle) of bifurcation curves that determine the dynamics of the Lorenz attractor and shape its existence region. The bundle is bordered by two curves: LA, bounding the red region from below, corresponds to the formation of the Lorenz attractor. The other curve, 2HB, on the border between the light-blue region and multicolored region of chaos, corresponds to a double pulsed homoclinic loop [Shilnikov, 1993; Shilnikov *et al.*, 1993]. The inclination-switch bifurcation of this loop plays a critical role in the transformation of the Lorenz attractor with no stable periodic

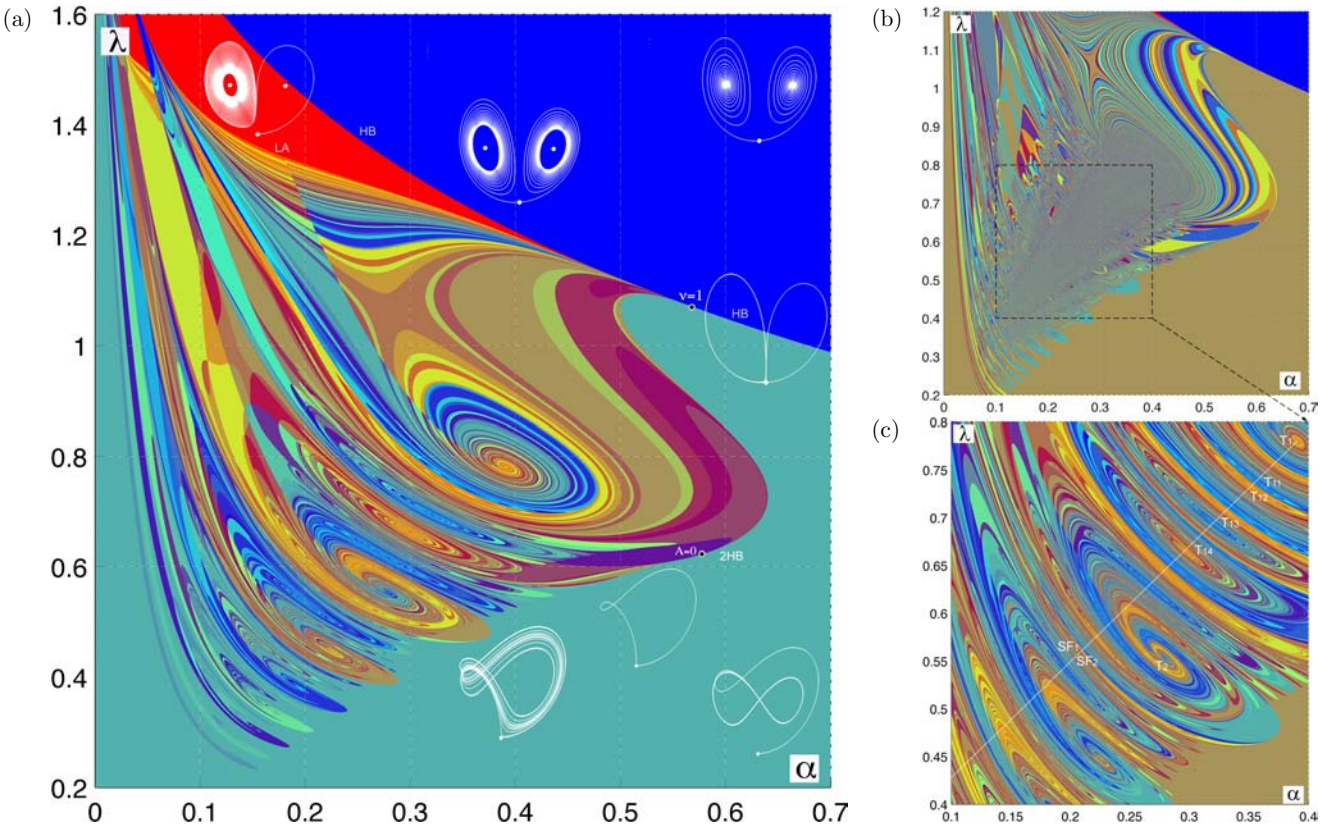

Fig. 5. (a) (α, λ)-sweep of the SM model using the {5–15}-kneading range. Solid-color regions, associated with constant values of the kneading invariant, correspond to simple dynamics dominated by stable equilibria (blue and red) or stable periodic orbits (light blue). The borderline between blue and red/light blue region corresponds to the bifurcation curve, HB, of the homoclinic butterfly. The merger point corresponding to a resonant saddle of codimension-two gives rise to loci of bifurcation curves bounding and foliating the region of the Lorenz attractor. This region contains a variety of swirls of various scales centered around Bykov T-points for heteroclinic connections as well as the saddles separating them. The line, 2HB, represents a bifurcation curve of a double-pulsed [10] homoclinic loop with codimension-two inclination-switch point, $A = 0$, on it. (b) Note saddles bounding codimension-two points in the diagram. High-resolution sweep of {12–22}-kneading range revealing fine foliation of the chaos region by homoclinic curves before the primary T-point at $(0.3903, 0.7805)$. Complex organization of multifractal swirls only appears noisy due to superabundant color variations in the given range. (c) Magnification depicting a plethora of embedded homoclinic swirls around T-points of various scales.

orbits into a quasi-hyperbolic one with stable orbits (in stability windows).

This diagram is a demonstration of this new computational approach. A feature of complex, structurally unstable dynamics is a dense occurrence of homoclinic bifurcations, which are represented by curves of various colors that foliate the chaotic region in the bi-parametric scan. We stress that given the depth (10 kneadings) of the scanning and the resolution of the colormap, the diagram can potentially reveal up to 2^{10} distinct bifurcation curves of homoclinic trajectories up to the indicated length. The top right picture in Fig. 5 presents a bi-parametric sweep of the same region, using a longer tail, {12–20}, of the kneading sequence. The sweep reveals fine organization structures foliating the existence region of the Lorenz attractors with bifurcation bundles, as well as two pronounced saddles separating the loci that converge to the primary T-point. They also show a "turbulent plume" made of swirling bifurcation structures originating from the primary T-point. The plume appears noisy due to color alternations and excess low-scale details. In what follows, we will focus on the complex self-similar organization and interconnection of such bifurcation structures centered around subsequent T-points.

5. Self-Similarity of Homoclinic Swirls

The bi-parametric sweep in Fig. 6 explores a fractal self-similar organization of bifurcation swirls,

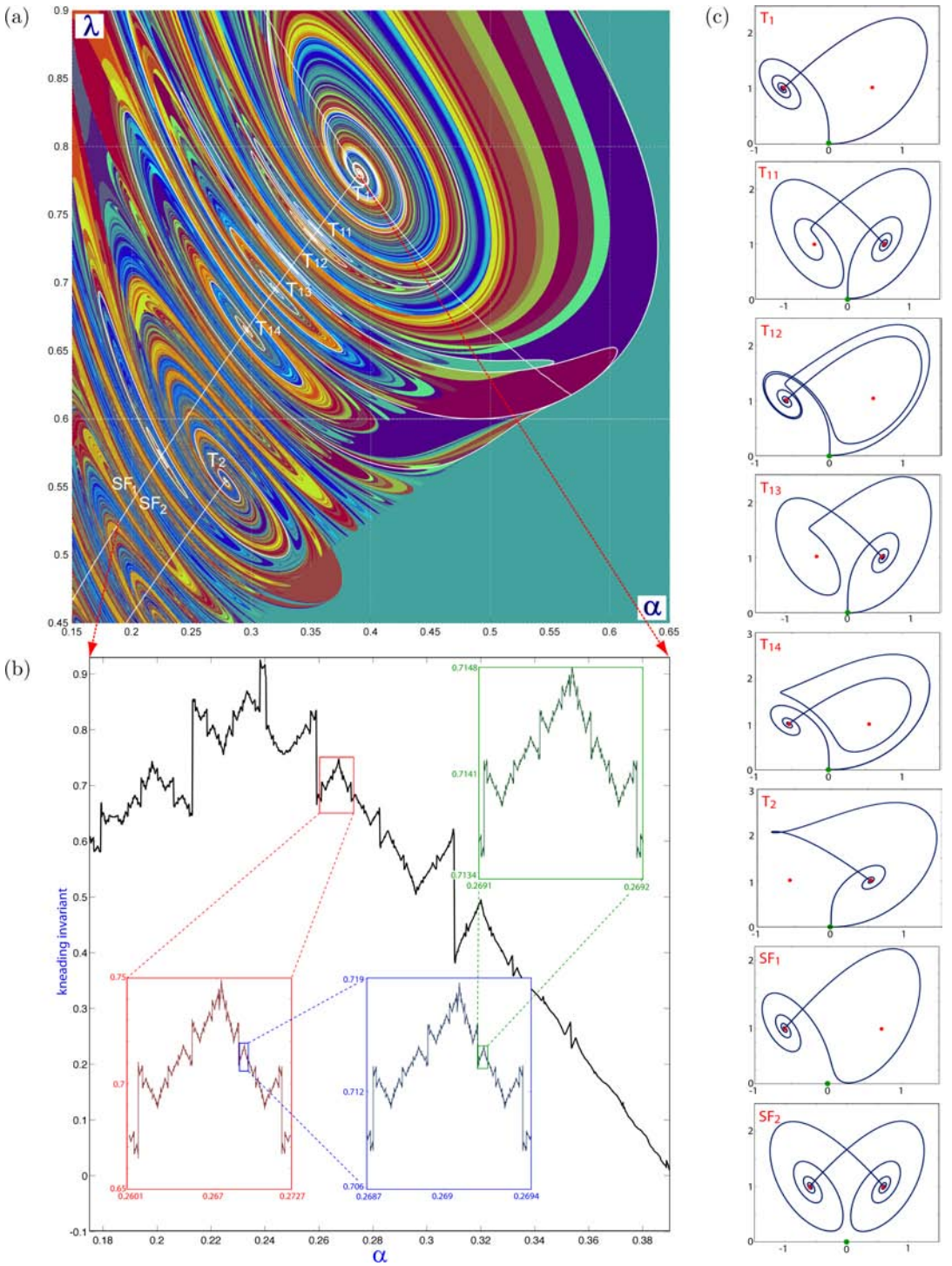

Fig. 6. (a) Bi-parametric sweep of {6–20}-kneading range revealing fractal structures of homoclinic bifurcation swirls parented by the primary T-point, $T_1(0.3903, 0.7805)$ with superimposed white bifurcation curves of separatrix loops obtained by the parameter continuation. Compare its self-similar structure with Bykov's unfolding in Fig. 2. (b) Self-similarity in the kneading dependence along the T-point pathway secluded between the curves SF_1 and SF_2 standing for homoclinic and heteroclinic connections of the saddle-foci. Critical and discontinuity points correspond to T-points and homoclinic bifurcations of the saddles shown in the side panels. (c) Various heteroclinic and homoclinic connections corresponding to the bifurcations selected in the bi-parametric sweeps shown in Fig. 5 and in the left panel: T_1 — the primary T-point of $\{1, 0^\infty\}$-type; SF_1 and SF_2 — homoclinic and heteroclinic saddle-foci; T_{1k}, $k = 1, 2, \ldots$ parented by T_1 and nested between SF_1 and SF_2; T_2 — secondary T-point of $\{1, 0, 1^\infty\}$-type and its subsidiaries.

which are centered around subsequent T-points. These points, including the secondary one, T_2 at $(0.2784, 0.5543)$, are parented by the primary one, $T_1(0.3903, 0.7805)$, located at right-top corner of the left panel. One can see that the diagrams disclose all details of the bifurcation structures of the Bykov T-points [Bykov, 1980]. Fine structures of the bi-parametric scan can be enhanced further by examining longer tails of the kneading sequences. This allows for the detection of smaller-scale swirling structures within the homoclinic scrolls, as predicted by theory (Fig. 2). From it we know that the subsidiary/peripheral points, T_{1k}, parented by the primary one, T_1, must nest within an ultra thin wedge bordered by the bifurcation curves corresponding to an initial homoclinic loop of either saddle-focus and a heteroclinic connection between both saddle-foci. To figure out a fractal hierarchy for the embedded swirls, we take a one-parameter sweep of the kneading invariant along a T-point pathway. The result is shown in the bottom panel in Fig. 6. The right end point at $\alpha = 0.3903$ in the diagram corresponds to the primary T-point. In it, local maxima and minima are associated to subsidiary T-points, while discontinuous points mark homoclinic bifurcations at which the kneading abruptly jumps in value. This diagram allows one to evaluate a renormalization factor of the fractal line. We can conjecture that the turbulent transition of homoclinic swirls is imperative for homoclinic bifurcation curves, which cannot cross each other, to embed into the compact region of chaotic dynamics in the SM model. In this region, chaotic dynamics in the SM model due to the Lorenz attractor are additionally amplified by spiral chaos due to Shilnikov's saddle-foci. Such chaos in the parameter space caused by the abundance of T-points, and due to interaction of the homoclinics of the saddle and saddle-foci, and contrasts vividly to a well parameterized foliation of the existence region of the Lorenz attractor above the primary T-point. Next we will analyze the way the foliation breaks down on a boundary below which the Lorenz attractor transforms into a quasi-chaotic attractor coexisting with stable periodic orbits with narrow attraction basins. Note that alternation of stability windows with stable periodic orbits and chaos is a feature of systems with saddle-foci and sign constant divergence like the model under consideration.

6. Inclination-Switch Bifurcations

In [Shilnikov, 1968a], L. P. Shilnikov introduced the conditions giving rise to bifurcations of codimension-two termed as orbit-flip and inclination-switch (Fig. 3) that can only occur in 3D+ systems. Besides that, the inclination-switch bifurcation even in the case of an expanding saddle with the saddle index satisfying the condition $1/2 < \nu < 1$ can also lead to the onset of stable orbits in the phase space of systems. As such, the occurrence of such a bifurcation is an alarming sign for the Lorenz attractor in the SM-model. Below we will outline the essence of the inclination-switch bifurcation. Its in-depth analysis is given in [Shilnikov *et al.*, 1998, 2001].

Figure 7 illustrates the concept of an inclination-switch bifurcation, which gives rise to the emergence of a stable orbit. The setup is the following: the 1D separatrix Γ^+ of the saddle of type $(2, 1)$ comes back to the saddle along the [vertical] leading direction. We explore the global map that takes a cross-section, Π, transverse to the stable manifold, W^s, onto itself along the homoclinic loop. Typically, the local map near the saddle is an expansion for $\nu < 1$, i.e. it must stretch a square or a volume. Figure 7 sketches how the local map takes a small interval $d_1 \ll 1$ on Π into $d_2 \sim d_1^\nu > d_1$. Let us picture an evolution, along the separatrix loop, of a piece, $\mathfrak{M}$, of a leading manifold, being defined locally and tangent to a span of the eigenvectors corresponding to the leading stable and unstable characteristic exponents, $s_2 < 0 < s_1$, respectively, of the saddle. As $\mathfrak{M}$ is dragged away from the saddle by the outgoing separatrix, it starts curving so that it hits the cross-section, Π, with a transversally squeezed hook due to the strongly stable exponent, $s_3 < s_2$. Because of bending, the image of d_2 becomes shorter than the original, d_1, i.e. $\mathrm{T}\, d_1 < d_1$ which was not the case prior to the bifurcation when the overall map was a stretching one. In the aftermath of bending, the global map T becomes a contraction after it overcomes the persistent stretching effect of the local map near the saddle. This map makes the image $\mathrm{T}\Pi_1$ of the right (relative to the stable manifold, W^s, of the saddle) portion, Π, of the cross-section stretch and bend, so that it looks like a hook or a Smale horseshoe. As such, the map may gain stable fixed points coexisting along with saddle periodic ones.

The 2D return map near the primary homoclinic butterfly of two separatrix loops of a saddle is

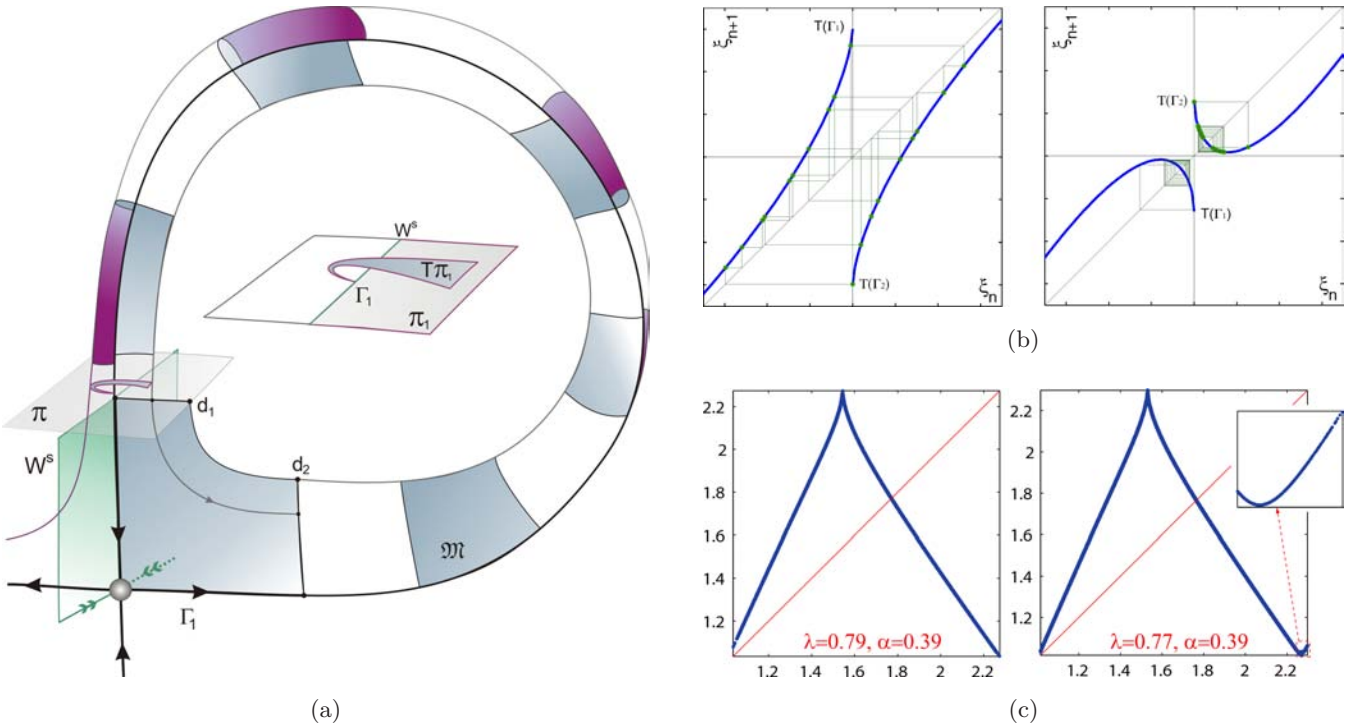

Fig. 7. (a) Geometry of an inclination-switch homoclinic bifurcation causing the emergence of stable orbits near the saddle with a saddle index $\nu < 1$. Its core element is local expansion ($d_1 < d_2 \sim d_1^{\nu}$) of an area, $\mathfrak{M}$ between a 1D outgoing separatrix Γ^+ and a close trajectory. This is further followed by bending such that the global return map T takes a cross-section Π, transverse to a 2D stable manifold of the saddle, becomes a contraction with stable fixed points, rather than an expansion generating saddle fixed points. (b) 1D discontinuous Lorenz map (4) without and with bending, respectively, prior to and after the inclination-switch bifurcation. Progressive bending gives rise to a saddle-node bifurcation, followed by a cascade of period-doubling bifurcations, followed by a secondary homoclinics as soon as the graph, $T\Pi_1$ lowers below the ξ_n-axis. (c) The evolution of the cusp-shaped graph of the 1D-map generated by critical points of the z-coordinate of a chaotic trajectory on the Lorenz attractor in the SM-model above and below the boundary $A = 0$, (Fig. 8) resulting in the formation of the characteristic hook (bend).

a core of the geometric model of the Lorenz attractor proposed in [Afraimovich *et al.*, 1983]. The map is supposed to meet a few analytical conditions guaranteeing that a system in question possesses a genuine chaotic attractor without stable orbits and homoclinic tangencies. A violation of the conditions occurs on a boundary of its existence region. Near the aforementioned codimension-two bifurcations the 2D map can be further reduced to a simplified 1D map (Fig. 7) in the following form [Shilnikov *et al.*, 1998, 2001]:

$$\xi_{n+1} = [\mu + A|\xi_n|^{\nu} + o(|\xi_n|^{2\nu})] \cdot \mathrm{sign}(\xi_n), \quad (4)$$

here $1/2 < \nu = |\lambda_2|/\lambda_1 < 1$ is the saddle index, locally μ controls the distance between a separatrix, Γ^+, and the stable manifold, W^s of the saddle at the origin, and A is the separatrix value [Shilnikov, 1993]. The term $o(|\xi_n|^{2\nu})$ is no longer negligible whenever $|A| \ll 1$ near the inclination-switch bifurcations. The top right panels in Fig. 7 illustrate the geometry of the map for positive and negative A. One can figure from the geometry of the hooked map that the unfolding an inclination-switch bifurcation must include saddle-node (tangent) and period-doubling bifurcations of fixed points, as well as double homoclinics. Say, if the inclination-switch occurs at the homoclinic loop with the [10] kneading, there will be a couple of bifurcation curves of double homoclinics, [10.10] and [10.01] emerging from the codimension-two points. An alternative, though expensive, solution for locating the curve $A = 0$ in the parameter space is by detecting the hooks in the return map generated by successive minima of the z-variable. Two such maps above and below the curve $A = 0$ at two locations, $\alpha = 0.39$, and $\lambda = 0.79$ and $\lambda = 0.77$, are presented in the bottom right panel of Fig. 7. The latter map features a second smooth critical point in addition to the cusp that will break down the instability and lead to the occurrence of

stable periodic orbits in the phase space and stability windows in the parameter space of the SM-model. We note that at lower λ and α values there are other curves similar to $A = 0$ [Shilnikov *et al.*, 1993]. Crossing down each such curve makes the return map bend again to gain additional turns. With every new turn, the map near the saddle starts appearing like the Poincaré map near a Shilnikov saddle-focus. The distinction though is that the spiraling saddle-focus map generates countably many Smale horseshoes, whereas the map near such twisting saddle has only a finite number of turns.

7. Shilnikov Flames

The geometry of the formation of homoclinic hooks in Fig. 7 suggests a computational algorithm for detecting the boundary in the parameter space of the model beyond which the system may have stable orbits along with the Lorenz attractor [Bykov & Shilnikov, 1989, 1992; Shilnikov, 1991, 1993]. The algorithm takes into consideration the behavior of two trajectories: the separatrix itself and close one above it because the leading direction at the saddle here is the z-axis. The (orange) curve of the hook formation is denoted by $A = 0$ in Fig. 8, thus symbolizing the original concept — the zero separatrix quantity A [Shilnikov, 1967a]. Above (below) the curve, $A > 0$ ($A < 0$) and hence all separatrix loops that are orientable become nonorientable. Its intersection points with the corresponding homoclinic curves correspond to codimension-two inclination-switch bifurcations, the sequence of which begins with the very first point on the curve, labeled [10] in Fig. 8, standing for the double homoclinic loops.

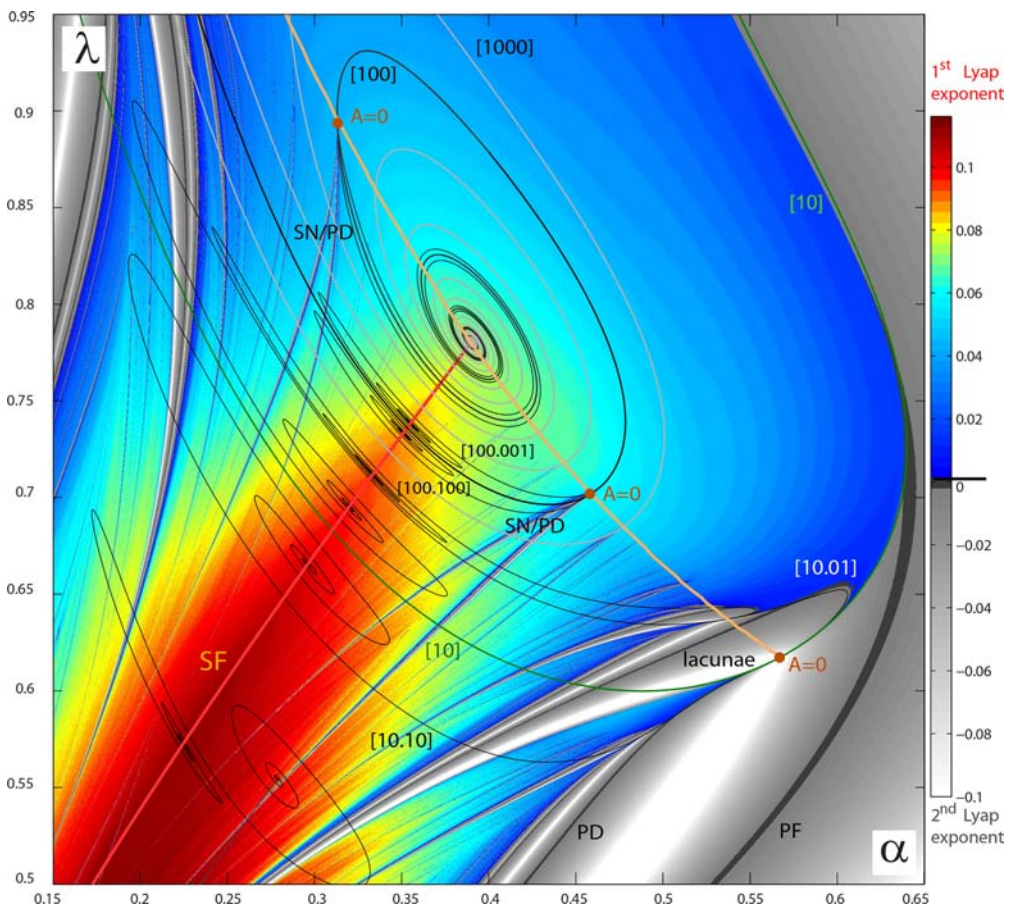

Fig. 8. Biparametric LE-sweep overlaid with homoclinic (black) and heteroclinic (red) bifurcation curves. Gray shades and colors are associated with LE quantities: $\lambda_2 < \lambda_1$. Major Shilnikov flames containing stability windows adjacent to codimension-two inclination-switch bifurcations (dots) on the (orange) curve, $A = 0$, demarcating the boundary of the existence region of the Lorenz attractor in the (α, λ)-parameter plane; the SN, PF and PD labels identify saddle-node, pitch-fork and period-doubling bifurcations. Superimposed black lines are several principal bifurcations curves of separatrix loops, which are obtained by the parameter continuation. Note a bifurcation pathway connecting two T-points.

In Fig. 8, we present a biparametric LP-sweep of the SM-model near the primary T-point to study the transition from the existence region of the Lorenz attractor to the regions of quasi-chaotic dynamics with inclusions of stability windows. Areas with gray shadows stand for the regular dynamics due to the presence of stable periodic orbits, for which $\lambda_2 < 0$, $\lambda_1 = 0$. Here, dark gray lines indicate bifurcations, saddle-node (SN), pitch-fork (PF) and period-doubling (PD), where λ_2 approaches zero from below. The colored regions stand for chaotic dynamics with $\lambda_1 > 0$; particularly, colors in the spectrum are associated with a range of λ_1 positive values. This diagram is superimposed with several homoclinic and heteroclinic bifurcations curves obtained by the parameter continuation technique. The abbreviation SF stands for the bifurcation curves of Shilnikov saddle-foci around which (red zone) the Lyapunov exponent is maximized. Labels [100], [10.01] based on kneading notations, stand for bifurcation curves of homoclinic loops spiraling toward the T-point. Several dots, labeled $A = 0$, mark the locations of codimension-two inclination-switch bifurcations on the (orange) curve below the hook formation that gives rise to the depicted homoclinic curves. The curve $A = 0$ demarcates the boundary of the existence region of the Lorenz attractor leading to its termination and giving rise to the emergence of stable periodic orbits. Such orbits exist and bifurcate within stability windows, called *Shilnikov flames*. Each such flame originates from a codimension-two homoclinic bifurcation that occurs at the intersection point of a homoclinic bifurcation curve with the curve $A = 0$. Since the Lorenz attractor is structurally unstable, homoclinic bifurcation curves densely foliate its existence region [Fig. 5(a)], and produces countably many codimension-two inclination-switch points on $A = 0$. Loosely speaking, the physical length of homoclinic loops can be viewed as the order number of the Shilnikov flames, which are bigger the lower the order number. Several such flames are revealed in Fig. 8: the largest ones originate from the inclination-switch bifurcations (on $A = 0$) corresponding to the shortest homoclinic loops, symbolically encoded as [10], [100], [10.01], etc. The left panel in Fig. 9 enlarges the Shilnikov flame at the crossing of $A = 0$ and the [100]-homoclinic loop, while the right panel presents a one-parameter bifurcation diagram along the vertical (red) λ-segment cross-cutting through the flame. Both unambiguously reveal the inner bifurcation organization of the flame including saddle-node bifurcations (Fig. 8) followed by a period-doubling cascade and secondary bifurcations of homoclinic loops, here [100.100] and [100.001]. One can see from Fig. 8 that the homoclinic bifurcation curves spiral up onto the matching T-points. The saddle-node

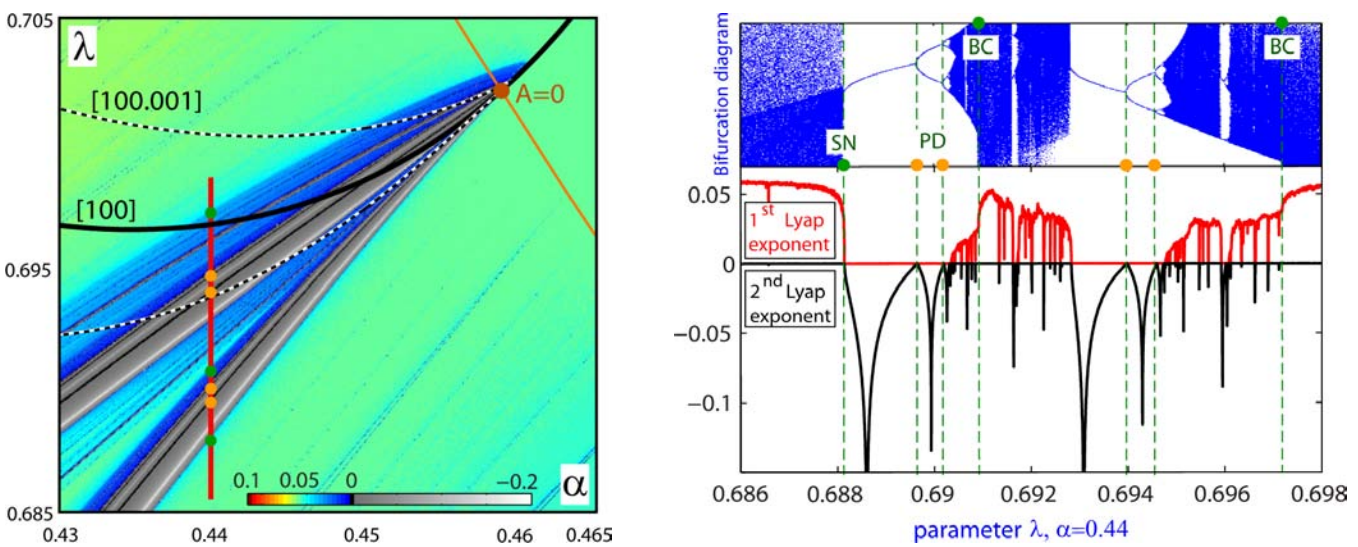

Fig. 9. (Left) LE-sweep magnification of a Shilnikov flame near the codimension-two point of the [100]-homoclinic loop revealing the fine organization of the bifurcation unfolding and the stability windows. (Right) One-parameter cut through the Shilnikov flame [depicted in panel (a)] disclosing cascades of saddle-node and period-doubling bifurcations within it, as well as the occurrence of the secondary, [100.100] and [100.001], homoclinics.

bifurcations bound the margins of the stability windows, and a period-doubling cascade within, which are all typical for quasi-attractors — where a complex hyperbolic trajectory structure coexists or becomes intermittent with stable periodic orbits. These nonlocal bifurcation puzzles agree well with the Bykov theory of T-points illustrated in Fig. 2 and the theory of codimension-two homoclinic bifurcations [Shilnikov *et al.*, 1993, 1998, 2001]. As such, the curve $A = 0$ sets a borderline demarcating the existence region of the Lorenz attractor from below in the (α, λ)-parameter space [Shilnikov, 1993].

8. Wild Chaos in Phase and Parameter Space

In the region below the curve $A = 0$, the dynamics of the SM-model becomes wildly unpredictable. Here, we use two senses of the term "wild." One is that the chaotic dynamics due to the Lorenz attractor are amplified by spiral chaos due to the Shilnikov saddle-foci near the primary T-point pathway, SF, in the LE-diagram in Fig. 8. This leads to onsets of *quasi-chaotic* attractors, the paradigm of which was introduced and developed by L. P. Shilnikov within the framework of the mathematical chaos theory [Afraimovich & Shilnikov, 1983; Shilnikov, 1997, 2002]. Such a chaotic set is impossible to parameterize and hence to fully describe its multicomponent structure due to dense complexity of ongoing bifurcations occurring within it [Bykov, 1993]. The complexity of the bifurcation structure of the Lorenz-like systems in regions of quasi-attractors is a perfect illustration of this paradigm. This is a second sense of the term wild: unlike the well-foliated existence region of the Lorenz attractor by bundles of bifurcation curves, the region of quasi-attractors is intricately stirred by T-points of various scales, and mixed with stability windows corresponding to stable periodic orbits emerging and vanishing as the parameters are varied.

In terms of the Lyapunov exponents quantifying instability of trajectory behaviors, the direct indication of intensifying disorder is the presence of a red(ish) zone around the pathway where the positive (largest) LE is maximized, compared to the cold (blue) chaos of the Lorenz attractor. In the wild-chaos region, bifurcations of homoclinic and periodic orbits become totally unpredictable [Gonchenko *et al.*, 1996]. One can see from Fig. 5(b) showing the {12–22}-kneading scan of the SM-model that the parameter region below the primary T-point appears quite noisy. The "parameter turbulence" created and stirred by homoclinic swirls of various scales makes it hard to find two points in this region with the same kneading value. Below we will present and discuss a few cases of interesting parameter structures revealed by this kneading toolbox. We remind the Reader that these are homoclinic structures made of separatrix loops of finite lengths (no more than 50 kneadings).

The first in the list is an organization of a fractal boundary between the regions of chaos and simple dynamics due to stable periodic orbits; the latter is color-coded with gray in Fig. 4 and in light-blue in Fig. 5(a). Let us reiterate that the kneading toolbox designed for homoclinic bifurcations does not detect local bifurcations of stable periodic orbits. As such, the region of trivial dynamics looks solid blue without any trace of pitch-fork,

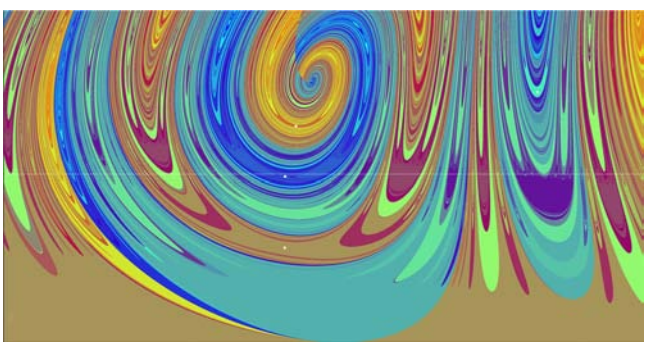

(a)

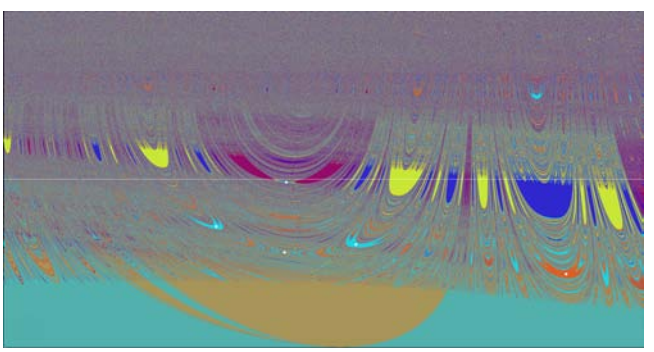

(b)

Fig. 10. Magnification of the vicinity of the T_2-point at two different resolutions: (a) {6–20} and (b) {17–20}-kneading ranges revealing a fine structure and self-similarity of the fractal border between the regions of simple dynamics (solid color) and complex chaotic dynamics. White dots mark locations of saddles.

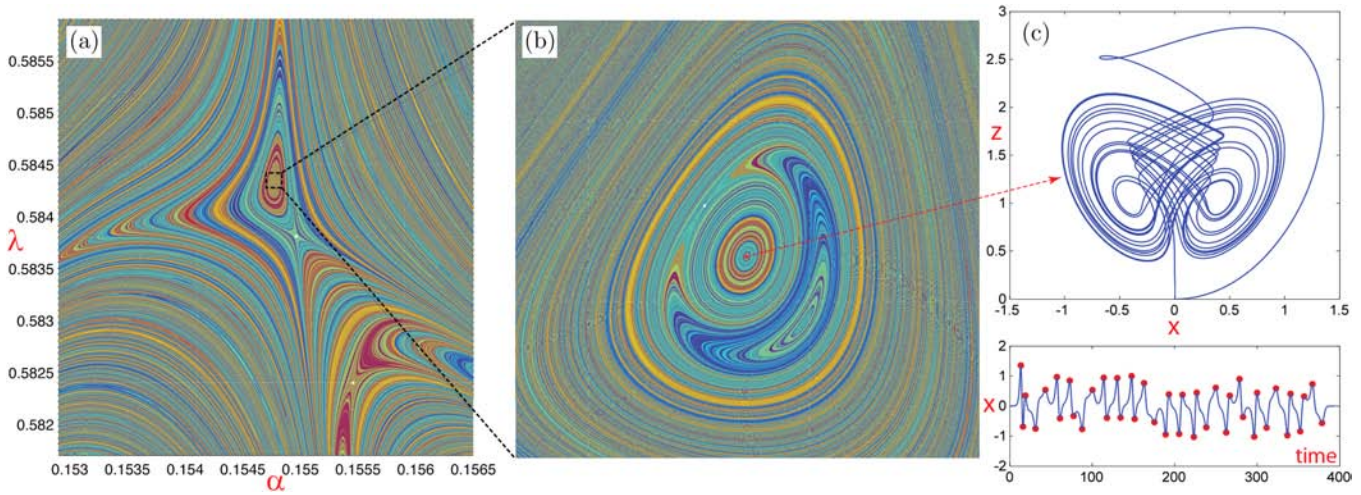

Fig. 11. (a) Embedded centers and saddles (white dots) in the parameter plane fragment. Scan of {20–35}-kneading range. (b) Magnification of the center region with a fine arrangement of self-similarity of long flip-flops of homoclinic bifurcations. Scan of {25–40}-kneading range. (c) Long flip-flop homoclinic connection at ($\alpha = 0.1548, \lambda = 0.5843$) corresponding to the center point.

saddle-node or period-doubling bifurcations that are known to occur there, as we can see from Fig. 4. Figure 10 focuses on a fragment of the kneading scan in the vicinity of the T_2-point (Fig. 6) near a border between the region of simple dynamics (solid color), dominated by stable periodic orbits and chaos. Its panels, presenting two resolution scans of {6–20} and {17–20}-kneading range, reveal self-similar structures that constitute a fractal border. On the border, a chaotic attractor undergoes an intrinsic crisis and breaks into two asymmetric ones emerging through period-doubling cascades [Shilnikov, 1986, 1993], just like the Lorenz model at large Rayleigh numbers [Robins, 1979; Franceschini, 1980]. In terms of the 1D bended maps depicted in Fig. 7, this occurs when the critical points cross the horizontal axis, which lets trajectories, which used to be trapped on either side of the unimodal graph of the map, switch between both branches thus filling in a symmetric chaotic attractor.

8.1. *Elliptic islands and saddles*

In the region of wild dynamics there are a variety of curious homoclinic bifurcation phenomena that are revealed by the symbolic toolkit. They are by-products of swirling patterns due to T-points, which can be viewed as "dissipative" structures in the parameter space. In contrast, "conservative" (looking) structures are comprised of elliptic islands separated by saddles, as the ones shown in Fig. 11. An elliptic island appears as a collection of concentric rings. Unlike T-points, each ring is a closed level curve corresponding to a long homoclinic loop with a kneading that does not change along the ring. Increasing the kneading resolution lets one obtain deeper insight into the organization of elliptic islands in the parameter plane. It turns out that, like T-points, there is another self-similar organization of embedded saddles and non-nested centers on smaller scales within which may appear to be outer rings [Fig. 11(b)]. The closer one approaches a center of the rings, the greater the number of flip-flops and twists the outgoing separatrix makes before returning to the saddle at the origin. As in the case of conservative dynamics, a saddle in the parameter plane sets a threshold between level curves of constant kneadings.

9. "Saddle-Node" Bifurcations in 3D-Parametric Sweeps

Homoclinic bifurcation curves disclosed by the computational toolkit can be viewed as level curves of constant kneading values. Recall that by construction (not counting the very first "+1"), the range of the kneading values is $[0, 1]$. Therefore, we can look at the kneading bifurcation diagrams from different angles, as in Fig. 12 depicting two fragments of the kneading *surface* in a 3D (α, λ, K)-parameter space; K from (3) denotes the kneading value. Now, T-points are viewed as local maxima and minima (vortices) separated by saddles. In the given context a saddle in the parameter plane is a

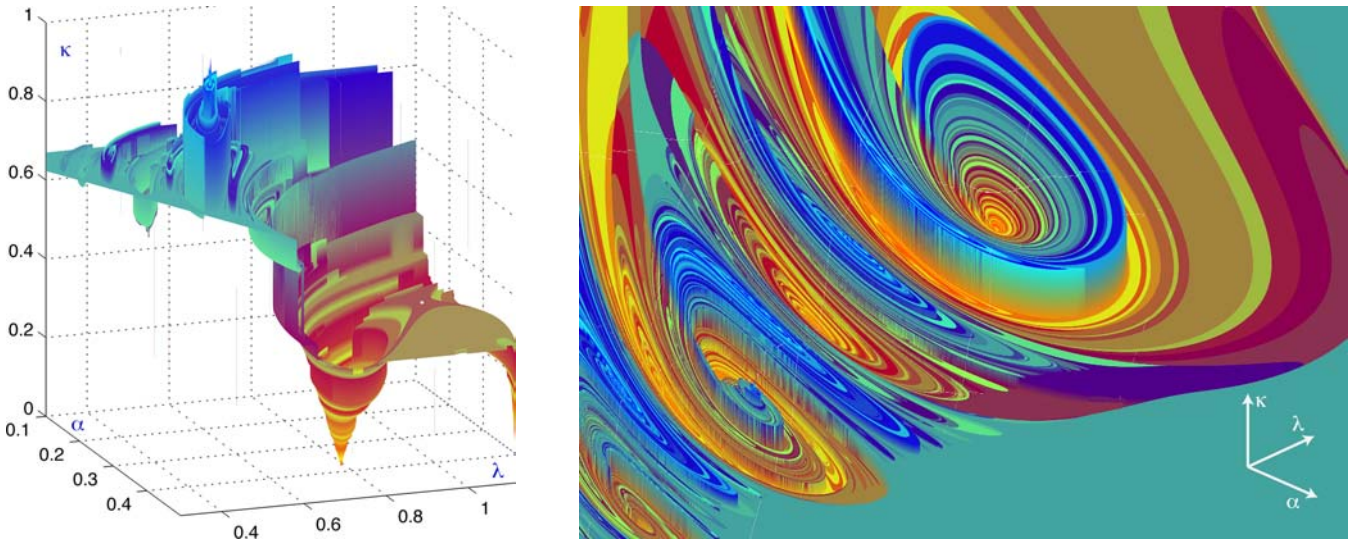

(a) (b)

Fig. 12. (a) Kneading surface depicting the vicinity of the primary T-point — A large vortex in the (α, λ, K)-parameter space, whose basin is bounded by a saddle (white dot). (b) Magnified fragment of the bifurcation surface near the primary T-point stirring the region of wild dynamics with multifractal organization; here is {5–15}-kneading range.

point at which two level curves corresponding to the same kneading touch and next swap, loosely speaking, such a surface can be visualized as a potential (in terms of physics) with noncrossing pathways other than at singularities — saddles and T-points, and other codimension-two points in the parameter space. This interpretation is useful for a forthcoming explanation of "bifurcations" of bifurcation

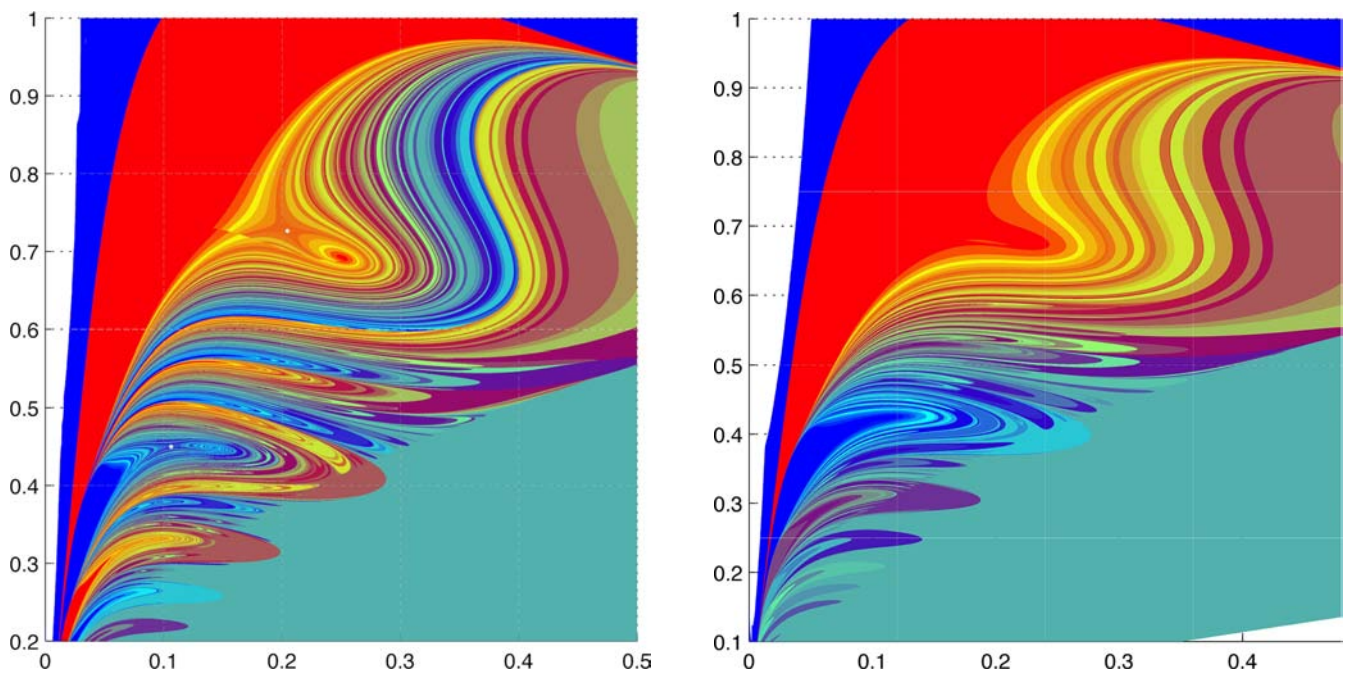

(a) (b)

Fig. 13. Two slices, at (a) $B = 0.11$ and (b) $B = 0.125$, of the 3D bifurcation diagram in the (α, λ, B)-parameter space, showing "saddle-node" bifurcations eliminating T-points merging with nearby saddles (white dots). The kneading range is {5–15}. Compare with Fig. 5 at $B = 0$.

curves in the SM-model (1) as the third parameter, B is varied. Recall that, up to now we have presented the results for $B = 0$.

Figure 13 depicts two slices, at $B = 0.05$ and $B = 0.11$, of the 3D bifurcation diagram in the (α, λ, B)-parameter space. The panels demonstrate the evolution of the original diagram in Fig. 5 as B is increased. One can see T-points vanishing with an increase of B through merges with nearby saddles, so that the chaos region will eventually be foliated by untwisting level curves originating from the codimension-two point corresponding to the resonant homoclinic saddle with a zero saddle value, and terminating at $(\alpha = \lambda = 0)$, which corresponds to a singular system with all three equilibria gathered at the origin. To draw a parallel with a saddle-node bifurcation of equilibria in a phase plane, one can speak of similar bifurcations of saddle and T-point structures in the parameter space that occur as the kneading surface rids of vertices and becomes "more flattened." Recall that like phase trajectories, homoclinic bifurcation curves do not cross and terminate at singularities — codimension-two points, like T-points, and the ones corresponding to resonant saddle and inclination-switch bifurcations.

10. Precursor of Inclination-Switching

In this final section we will try to rationalize the cause of inclination-switch bifurcations in the SM-model. An evidence or, vice-versa, a consequence of such a bifurcation is various cascades of period-doubling bifurcations that occur in flows, which, loosely speaking, generate bending return maps.

Let us consider the SM-model, at $B = 0$ for simplicity, in the singular limit $\alpha = 0$, where the z-variable becomes a control parameter:

$$\dot{x} = y, \quad \dot{y} = x - \lambda y - xz, \quad z \geq 0. \tag{5}$$

The stability of the only equilibrium state of this linear system (fast subsystem at $\alpha \ll 1$) depends on the height of z: $s_{1,2} = [-\lambda \pm \sqrt{\lambda^2 - 4(1-z)}]/2$. For $z < \lambda^2/4 + 1$, the origin is a saddle, while it becomes a stable focus at larger z-values. This will determine the dynamics of the system close to the z-axis when α is small. So, whenever the saddle has a homoclinic loop, depending on how high the returning separatrix Γ^+ climbs up in the phase space, it may turn around the leading stable direction — the z-axis. The number of turns

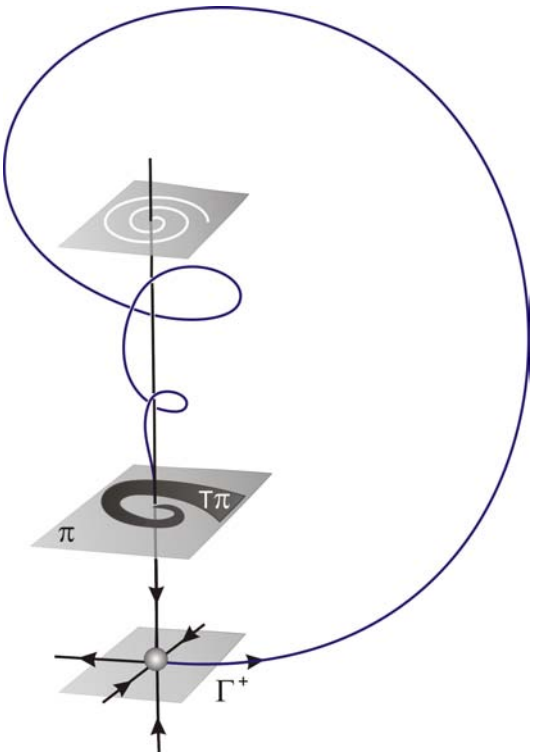

Fig. 14. Slow-fast dynamics around as a precursor of inclination-switch bifurcations in the SM-model. Sketch of a twisting flow making the separatrix of the saddle turn around the stable leading direction, the z-axis, and hence the return map, T, taking a cross-section Π into itself, looks like the genuine map near the Shilnikov saddle-focus.

depends on how long the separatrix Γ^+ follows the "spiraling" segment of the z-axis and on how strong the twisting flow is nearby, see the sketch in Fig. 14. Multiple inclination-switches help the homoclinic saddle pretend to be a genuine Shilnikov saddle-focus. This phenomenon, called extra-twisting, was also observed in the Lorenz model at small parameter values [Sparrow, 1982]. Such a twisting in the limiting case is a precursor of the inclination-switch bifurcations in the SM-model and other alike systems. An indirect answer to the question of whether a homoclinic loop is oriented or non-oriented (twisted) is basically determined by how high the returning separatrix goes while approaching the leading z-axis on the stable manifold of the saddle at the origin.

11. Conclusions

This paper presents a case study on organizations of homoclinic bifurcations in the parameter space segment corresponding to the Lorenz strange attractor in the Shimizu–Morioka model.

It sheds a light on the pivotal role of homoclinic and heteroclinic bifurcations as emergent centers for pattern formations in parameter spaces corresponding to complex dynamics. It also reveals universal principles of chaotic dynamics in deterministic systems with Lorenz-like attractors, which include the Lorenz equation itself and similar models [Barrio *et al.*, 2012, 2013; Xing *et al.*, 2014a; Xing *et al.*, 2014b]. All these systems feature various codimension-two heteroclinic and homoclinic bifurcations such as Bykov T-points, resonant saddles and inclination-switching. We have demonstrated mechanisms generating Shilnikov flames, which underlie the bifurcation transitions from the Lorenz attractor to wildly chaotic quasi-attractors, and outline multifractal organizations of the corresponding regions in the parameter space. Our numerical experiments with kneading-based scans of several Lorenz-like systems have unambiguously revealed a wealth of multiscale swirling and saddle structures occurring in intrinsically fractal regions corresponding to strange chaotic attractors with Shilnikov saddle-foci in diverse systems. This original computational method based on kneading invariants will greatly benefit in-depth studies of an array of other systems with homoclinic chaotic dynamics, that support the introduction of symbolic partitions.

On a technical side, we note that with the use of GPU parallel simulations and optimized Taylor expansion ODE integrators, the time needed for completion of exhausting bi-parametric kneading scans of extra high-resolutions can be feasibly reduced by an order.

The Reader can find multimedia versions of the evolution of the bifurcation diagrams of the SM-model at this link https://www.youtube.com/watch?v=P-X5vpyHTJ4. A gallery of kneading scans © of the Shimizu–Morioka, Lorenz, Homoclinic Garden and other models is located at http://www.ni.gsu.edu/~ashilnikov/chaosquest. Copyrighted high-resolution images are available upon request.

Acknowledgments

PhD research of T. Xing was funded by NSF Grant DMS-1009591. R. Barrio was in part supported by Spanish Research project MTM2012-31883. A. Shilnikov was in part supported by NSF DMS-1009591 and RFFI 11-01-00001. His research is also partly supported by the grant in the agreement of August 27, 2013 No. 2.B.49.21.0003 between the Ministry of education and science of the Russian Federation and Lobachevsky State University of Nizhny Novgorod. We thank GSU students J. Collens, M. Crowe, R. Jetter, D. Knapper and A. Noriega for proof-reading and helpful suggestions, and V. Afraimovich, A. Neiman, D. Turaev, J. Wojcik and M. Zaks for helpful discussions, and R. Clewley for his guidance on the PyDSTool package [Clewley *et al.*, 2006] used in simulations.

References

Afraimovich, V. & Shilnikov, L. [1974] "On some global bifurcations connected with the disappearance of a fixed point of saddle-node type," *Dokl. Akad. Nauk. SSSR* **219**, 1281–1285 (in Russian); English Translation [1974], *Sov. Math. Dokl.* **15**, 1761–1765.

Afraimovich, V., Bykov, V. & Shilnikov, L. [1977] "The origin and structure of the Lorenz attractor," *Sov. Phys. Dokl.* **22**, 253–255.

Afraimovich, V. & Shilnikov, L. [1983] "Strange attractors and quasiattractors," *Nonlinear Dynamics and Turbulence*, Interaction Mech. Math. Ser. (Pitman, Boston, MA), pp. 1–34.

Afraimovich, V., Bykov, V. & Shilnikov, L. [1983] "On structurally unstable attracting limit sets of Lorenz attractor type," *Trans. Moscow Math. Soc.* **44**, 153–216.

Afraimovich, V. & Shilnikov, L. [1991] "On invariant two-dimensional tori, their breakdown and stochasticity," *Amer. Math. Soc. Trans.* **149**, 201–212 [translated from *Methods of the Qualitative Theory of Differential Equations*, Gor'kov. Gos. University, pp. 3–25 (1983)].

Barrio, R., Shilnikov, A. & Shilnikov, L. [2012] "Kneadings, symbolic dynamics, and painting Lorenz chaos," *Int. J. Bifurcation and Chaos* **22**, 1230016-1–24.

Barrio, R., Blesa, F., Serrano, S., Xing, T. & Shilnikov, A. [2013] "Homoclinic spirals: Theory and numerics," *Progress and Challenges in Dynamical Systems* (Springer, Berlin, Heidelberg), pp. 53–64.

Bykov, V. V. [1980] "On the structure of bifurcations sets of dynamical systems that are systems with a separatrix contour containing saddle-focus," *Methods of Qualitative Theory of Differential Equations*, Gorky University (in Russian), pp. 44–72.

Bykov, V. & Shilnikov, A. [1989] "Boundaries of the domain of existence of a Lorenz attractor," *Methods of Qualitative Theory of Differential Equations*, Gorky University (in Russian), pp. 151–159.

Bykov, V. & Shilnikov, A. [1992] "On the boundaries of the domain of existence of the Lorenz attractor," *Selecta Math. Soviet.* **11**, 375–382.

Bykov, V. V. [1993] "The bifurcations of separatrix contours and chaos," *Physica D* **62**, 290–299.

Clewley, R., Sherwood, W., LaMar, M. & Guckenheimer, J. [2006] "Pydstool: An integrated simulation, modeling, and analysis package for dynamical systems," Tech. Rep., http://pydstool.sourceforge.net.

Franceschini, V. [1980] "A Feigenbaum sequence of bifurcations in the Lorenz model," *Physica D* **3**, 397–406.

Gavrilov, N. & Shilnikov, L. [1972] "On three-dimensional dynamical systems close to systems with a structurally unstable homoclinic curve. I," *Sbornik*: *Math.* **14**, 467–485.

Gavrilov, N. & Shilnikov, L. [1973] "On three-dimensional dynamical systems close to systems with a structurally unstable homoclinic curve. II," *Sbornik*: *Math.* **19**, 139–165.

Glendinning, P. & Sparrow, C. [1986] "T-points: A codimension two heteroclinic bifurcation," *J. Stat. Phys.* **43**, 479–488.

Gonchenko, S. V., Shil'nikov, L. P. & Turaev, D. V. [1996] "Dynamical phenomena in systems with structurally unstable Poincare homoclinic orbits," *Chaos* **6**, 15–31.

Guckenheimer, J. & Williams, R. F. [1979] "Structural stability of Lorenz attractors," *Inst. Hautes Études Sci. Publ. Math.* **50**, 59–72.

Kaplan, J. L. & Yorke, J. A. [1979] "Preturbulence: A regime observed in a fluid flow model of Lorenz," *Comm. Math. Phys.* **67**, 93–108.

Lorenz, E. [1963] "Deterministic nonperiodic flow," *J. Atmosph. Sci.* **20**, 130–141.

Malkin, M. [1991] "Rotation intervals and dynamics of Lorenz type mappings," *Selecta Math. Soviet.* **10**, 265–275.

Milnor, J. & Thurston, W. [1988] *On Iterated Maps of the Interval*, Lecture Notes in Math., Vol. 1342, pp. 465–563.

Petrovskaya, N. & Yudovich, V. [1980] "Homolinic loops on the Saltzman–Lorenz system," *Methods of Qualitative Theory of Differential Equations*, Gorky University (in Russian), pp. 73–83.

Rand, D. [1978] "The topological classification of Lorenz attractors," *Math. Proc. Cambridge Philosoph. Soc.* **83**, 451–460.

Robins, K. [1979] "Periodic solutions and bifurcation structure at high r in the Lorenz model," *SIAM J. Appl. Math.* **36**, 457–472.

Robinson, C. [1989] "Homoclinic bifurcation to a transitive attractor of Lorenz type," *Nonlinearity* **2**, 495–518.

Rychlik, M. R. [1990] "Lorenz attractors through Šil'nikov-type bifurcation. I," *Erg. Th. Dyn. Syst.* **10**, 793–821.

Shilnikov, L. [1962] "Some cases of generation of periodic motions in an n-dimensional space," *Sov. Math. Dokl.* **3**, 394–397.

Shilnikov, L. [1963] "Some cases of generation of period motions from singular trajectories," *Mat. Sbornik* **61**, 443–466.

Shilnikov, L. [1965] "A case of the existence of a countable number of periodic motions," *Sov. Math. Dokl.* **6**, 163–166; Original: "On the case of existence of a countable set of periodic movements," *Dokl. Akad. Nauk SSSR* **160**, 558–561.

Shilnikov, L. [1967a] "The existence of a denumerable set of periodic motions in four-dimensional space in an extended neighborhood of a saddle-focus," *Sov. Math. Dokl.* **8**, 54–58.

Shilnikov, L. [1967b] "On a problem of Poincaré and Birkhoff," *Math. USSR Sb.* **3**, 353–371.

Shilnikov, L. [1968a] "On the birth of a periodic motion from a trajectory bi-asymptotic to an equilibrium state of the saddle type," *Sov. Math. Sbornik* **35**, 240–264.

Shilnikov, L. [1968b] "Structure of the neighborhood of a homoclinic tube of an invariant torus," *Sov. Math. Dokl.* **9**, 624–627.

Shilnikov, L. [1969] "On a new bifurcation of multidimensional dynamical systems," *Sov. Math. Dokl.* **10**, 1371–1389.

Shilnikov, L. [1970] "A contribution to the problem of the structure of an extended neighborhood of a rough equilibrium state of saddle-focus type," *Math. USSR Sb.* **10**, 91–102.

Shilnikov, L. [1980] "Bifurcation theory and the Lorenz model," Appendix to Russian edition of *The Hopf Bifurcation and Its Applications*, eds. Marsden, J. & McCraken, M., pp. 317–335.

Shilnikov, L. [1981] "The theory of bifurcations and quasiattractors," *Uspekh. Math. Nauk.* **36**, 240–242.

Shilnikov, A. [1986] "Bifurcations and chaos in the Morioka–Shimizu model. Part I," *Methods of Qualitative Theory of Differential Equations*, Gorky University (in Russian), pp. 180–193.

Shilnikov, A. [1989] "Bifurcations and chaos in the Morioka–Shimizu model. Part II," *Methods of Qualitative Theory of Differential Equations*, Gorky University (in Russian), pp. 130–138.

Shilnikov, A. [1991] "Bifurcation and chaos in the Morioka–Shimizu system," *Selecta Math. Soviet.* **10**, 105–117.

Shilnikov, A. [1993] "On bifurcations of the Lorenz attractor in the Shimizu–Morioka model," *Physica D* **62**, 338–346.

Shilnikov, A., Shilnikov, L. & Turaev, D. [1993] "Normal forms and Lorenz attractors," *Int. J. Bifurcation and Chaos* **3**, 1123–1139.

Shilnikov, L. [1994] "Chua's circuit: Rigorous results and future problems," *Int. J. Bifurcation and Chaos* **4**, 489–518.

Shilnikov, L. [1997] "Mathematical problems of nonlinear dynamics: A tutorial. Visions of nonlinear mechanics in the 21st century," *J. Franklin Instit.* **334**, 793–864.

Shilnikov, L., Shilnikov, A., Turaev, D. & Chua, L. [1998, 2001] *Methods of Qualitative Theory in Nonlinear Dynamics. Parts I and II* (World Scientific, Singapore).

Shilnikov, L. [2002] "Bifurcations and strange attractors," *Proc. Int. Congress of Mathematicians*, *Beijing* (*China*) (*Invited Lectures*) **3**, 349–372.

Shilnikov, L. & Shilnikov, A. [2007] "Shilnikov bifurcation," *Scholarpedia* **2**, 1891.

Shilnikov, L. & Shilnikov, A. [2008] "Shilnikov saddle-node bifurcation," *Scholarpedia* **3**, 4789.

Shimizu, T. & Morioka, N. [1980] "On the bifurcation of a symmetric limit cycle to an asymmetric one in a simple model," *Phys. Lett. A* **76**, 201–204.

Sinai, J. & Vul, E. [1981] "Hyperbolicity conditions for the Lorenz model," *Physica D* **2**, 3–7.

Sparrow, C. [1982] *The Lorenz Equations*: *Bifurcations*, *Chaos*, *and Strange Attractors*, Applied Mathematical Sciences, Vol. 41 (Springer-Verlag, NY).

Tigan, G. & Turaev, D. [2011] "Analytical search for homoclinic bifurcations in the Shimizu–Morioka model," *Physica D* **18**, 985–989.

Tresser, C. & Williams, R. [1993] "Splitting words and Lorenz braids," *Physica D* **62**, 15–21.

Tucker, W. [1999] "The Lorenz attractor exists," *C. R. Acad. Sci. Paris* **328**, 1197–1202.

Turaev, D. & Shilnikov, L. [1998] "An example of a wild strange attractor," *Sbornik. Math.* **189**, 291–314.

Vladimirov, A. & Volkov, D. [1993] "Low-intensity chaotic operations of a laser with a saturable absorber," *Opt. Commun.* **100**, 351–360.

Xing, T., Wojcik, J., Barrio, R. & Shilnikov, A. [2014a] "Symbolic toolkit for chaos explorations," *Int. Conf. Theory and Application in Nonlinear Dynamics* (*ICAND 2012*) (Springer International Publishing), pp. 129–140.

Xing, T., Wojcik, J., Zaks, M. & Shilnikov, A. [2014b] "Multifractal chaos: A hierarchical approach," *Chaos, Information Processing and Paradoxical Games*: *The Legacy of J. S. Nicolis*, eds. Nicolis, G. & Basios, V. (World Scientific, Singapore).